



Liquid phase separation and subsequent dendritic solidification of ternary $\text{Fe}_{35}\text{Cu}_{35}\text{Si}_{30}$ alloy

Sheng-bao LUO, Wei-li WANG, Zhen-chao XIA, Bing-bo WEI

Department of Applied Physics, Northwestern Polytechnical University, Xi'an 710072, China

Received 4 December 2015; accepted 12 April 2016

Abstract: Liquid $\text{Fe}_{35}\text{Cu}_{35}\text{Si}_{30}$ alloy has achieved the maximum undercooling of 328 K ($0.24T_L$) with glass fluxing method, and it displayed triple solidification mechanisms. A critical undercooling of 24 K was determined for metastable liquid phase separation. At lower undercoolings, α -Fe phase was the primary phase and the solidification microstructure appeared as homogeneous well-defined dendrites. When the undercooling exceeded 24 K, the sample segregated into Fe-rich and Cu-rich zones. In the Fe-rich zone, FeSi intermetallic compound was the primary phase within the undercooling regime below 230 K, while Fe_5Si_3 intermetallic compound replaced FeSi phase as the primary phase at larger undercoolings. The growth velocity of FeSi phase increased whereas that of Fe_5Si_3 phase decreased with increasing undercooling. For the Cu-rich zone, FeSi intermetallic compound was always the primary phase. Energy-dispersive spectrometry analyses showed that the average compositions of separated zones have deviated substantially from the original alloy composition.

Key words: undercooling; phase separation; dendritic growth; rapid solidification; solute distribution

1 Introduction

Liquid–liquid phase separation usually occurs in monotectic alloy system, which is immiscible in equilibrium. When a monotectic alloy melt is cooled into the miscibility gap, the homogeneous liquid alloy separates into two distinct liquids [1–3]. In the past few years, various research results have been published regarding the metastable liquid–liquid phase separation, which can be achieved only by undercooling the alloy melt. This phenomenon is the case for some peritectic alloy systems, such as Co–Cu [4,5] and Fe–Cu [6,7]. Up to now, the quantitative information and systematic analysis are limited for the phase selection and microstructural evolution during the metastable liquid phase separation of ternary alloys.

A third component was added into the binary alloy system to control the liquid phase separation [8,9]. Previous work reported that the addition of element Si into binary Fe–Cu alloy significantly affects the stability of liquid phase separation [10–12]. Binary $\text{Fe}_{50}\text{Cu}_{50}$ alloy exhibits a metastable phase separation process beyond a certain undercooling threshold, as reported in

Ref. [6]. Nevertheless, the addition of 4%–26% Si into binary $\text{Fe}_{50}\text{Cu}_{50}$ alloy induces a stable liquid phase separation, according to the liquidus projection of ternary Fe–Cu–Si alloy, as shown in Fig. 1 [13]. Meanwhile, it is reasonable to predict that a metastable liquid phase separation exists within the composition range of 0–4% and 26%– $x\%$ Si (x is a little more than 26) (mole fraction) added into binary $\text{Fe}_{50}\text{Cu}_{50}$ alloy. Therefore, the ternary Fe–Cu–Si alloy system is well suited for studying the influence of metastable liquid phase separation on the phase selection and microstructural evolution.

As mentioned above, metastable liquid phase separation takes place in undercooled alloy melts. In such a case, a large driving force for crystal growth is generated from the difference in Gibbs free energy between the metastable liquid phase and the solid phase. Consequently, rapid solidification takes place even with a slow cooling rate. Some distinct phenomena may occur during rapid solidification, for instance, competitive growth [14,15], microstructure refinement [16,17], solid solubility extension [18,19] or metastable phase formation [20]. Therefore, any investigation into metastable liquid phase separation under the non-equilibrium condition

should take into account the effect of rapid solidification. High undercooling can be obtained by several methods, such as glass fluxing [21], drop tube [22], electromagnetic levitation [23], and electrostatic levitation [24]. Among them, the glass fluxing method has the advantages of convenient operation, extensive applicability and obtaining substantial undercoolings for really bulk alloy melts.

In this work, the selected alloy is formed by adding 30% Si into binary $\text{Fe}_{50}\text{Cu}_{50}$ alloy to achieve metastable liquid phase separation. The chemical composition of $\text{Fe}_{35}\text{Cu}_{35}\text{Si}_{30}$ alloy lies outside the scope of the stable liquid phase separation [13], as presented by point *A* in Fig. 1. The substantial undercooling of this alloy is achieved by the glass fluxing method. As expected, the undercooled $\text{Fe}_{35}\text{Cu}_{35}\text{Si}_{30}$ alloy experiences a metastable liquid phase separation. The objective is to investigate the characteristics of liquid phase separation and subsequent dendritic growth within undercooled $\text{Fe}_{35}\text{Cu}_{35}\text{Si}_{30}$ alloy. These investigations help to reveal the solidification mechanism of undercooled multi-component alloys with metastable immiscible gap.

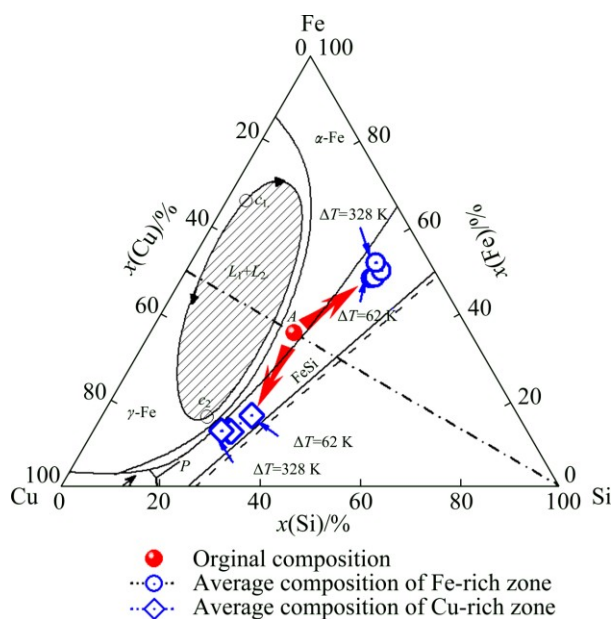


Fig. 1 Original composition and separated compositions of ternary $\text{Fe}_{35}\text{Cu}_{35}\text{Si}_{30}$ alloy at different undercoolings

2 Experimental

Ternary $\text{Fe}_{35}\text{Cu}_{35}\text{Si}_{30}$ alloy was arc melted from Fe (99.99% pure), Cu (99.99% pure) and Si (99.999% pure). The sample mass is about 1 g. An alloy sample was firstly placed in an alumina crucible, and then some Duran glass was used to cover the sample. The experiments were performed in a high-vacuum chamber. The alloy sample was heated by electromagnetic induction. After being superheated for 10–60 s, the alloy

melt was naturally cooled. The temperature was recorded by an infrared pyrometer, while the recalescence time was determined by a high-sensitivity photodetector.

After being sectioned and polished, the solidified samples were etched with a mixing solution of 5 g FeCl_3 , 5 mL HCl and 20 mL H_2O for about 15 s. The microstructure was investigated by a Zeiss Axiovert 200 MAT optical microscope (OM) and an FEI Sirion 200 scanning electron microscope (SEM). The phase identification was performed by a Rigaku D/max 2500 X-ray diffractometer. The solute distribution profile was detected by an Oxford INCA Energy 300 energy-dispersive spectrometer. Besides, the liquidus temperature of ternary $\text{Fe}_{35}\text{Cu}_{35}\text{Si}_{30}$ alloy was measured by a Beif WCR-2B differential thermal analysis calorimeter.

3 Results and discussion

3.1 Liquid phase separation and solute macro-segregation profile

Due to the lack of thermodynamic parameters for ternary $\text{Fe}_{35}\text{Cu}_{35}\text{Si}_{30}$ alloy, differential thermal analysis (DTA) was firstly performed. The liquidus temperature T_L of ternary $\text{Fe}_{35}\text{Cu}_{35}\text{Si}_{30}$ alloy is determined as 1395 K on the basis of the heating curve. In addition, no trace of liquid phase separation is found on both the cooling curve and the solidification microstructure of DTA sample. The undercooling ΔT is defined as $\Delta T = T_L - T_N$, where T_N is the nucleation temperature of the primary solid phase. Accordingly, the undercooling of DTA sample is determined to be 22 K. That is, liquid phase separation does not occur in the ternary $\text{Fe}_{35}\text{Cu}_{35}\text{Si}_{30}$ alloy if the undercooling is smaller than 22 K. This deduction is verified by the results in the glass fluxing experiments.

During the glass fluxing experiments, the achieved maximum undercooling for liquid $\text{Fe}_{35}\text{Cu}_{35}\text{Si}_{30}$ alloy is up to 328 K ($0.24T_L$). The alloy solidified at the undercooling of 22 K displays a dendritic morphology, which is shown in Fig. 2(a). If the alloy is undercooled to 24 K, liquid phase separation takes place. A small amount of Fe-rich liquid phase firstly separates from the homogeneous liquid and then gathers together at the sample bottom to form a Fe-rich zone, as illustrated in Fig. 2(b). Therefore, the undercooling threshold for metastable liquid phase separation can be taken as 24 K.

As the undercooling continues to increase, serious structural segregation takes place. The alloy melt separates into a Fe-rich liquid zone and a Cu-rich liquid zone. The Fe-rich liquid gradually floats toward the sample top, while the Cu-rich liquid sinks down to the sample bottom, as displayed in Figs. 2(c) and 2(d). Apparently, the evolution of macrosegregation is mainly

caused by the Stokes motion [25,26]. Figure 2(d) shows the macrostructural morphology of the alloy sample solidified at the maximum undercooling of 328 K. Clearly, the interface of the two segregated zones has evolved to be very smooth. This suggests that the extent of liquid phase separation has been improved at large undercoolings.

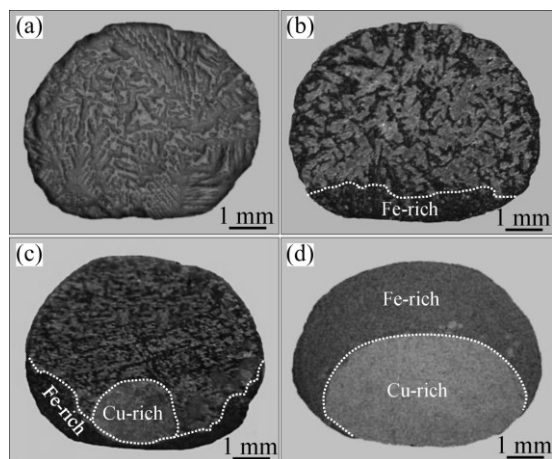


Fig. 2 Macrostructures of ternary $\text{Fe}_{35}\text{Cu}_{35}\text{Si}_{30}$ alloy solidified at different undercoolings: (a) $\Delta T=22$ K; (b) $\Delta T=24$ K; (c) $\Delta T=62$ K; (d) $\Delta T=328$ K

Due to the metastable liquid phase separation, the solute distribution within $\text{Fe}_{35}\text{Cu}_{35}\text{Si}_{30}$ alloy melt gradually varies with the enhancement of undercooling. The energy-dispersive spectrometry (EDS) analysis was performed to explore the solute redistribution profiles of macrosegregated alloy samples. In the present experiments, the undercooling range of these samples is from 62 to 328 K. The experimentally determined compositions of the Fe-rich and Cu-rich zones are marked by hollow circles and diamonds in Fig. 1, respectively. It is obvious that the separated compositions have deviated substantially from the original alloy composition. A segregation degree S_d is introduced to characterize the solute segregation of phase-separated zones:

$$S_d = \frac{c_{ps}}{c_o} \quad (1)$$

where c_{ps} is the actual solute content of the phase-separated zone, while c_o is the solute content of the original alloy. Figure 3 shows the solute segregation degree at different undercoolings. For the Fe-rich zone, the S_d of solute Si maintains a value of about 1.28 in the experimental undercooling range, while the S_d of solute Cu shows a declining tendency from 0.40 to 0.32 with increasing undercooling. In the Cu-rich zone, both the segregation degrees of solutes Si and Fe reduce with the enhancement of undercooling. In the experimental undercooling range of 62–328 K, the S_d of solute Si

reduces from an initial 1.0 to 0.86, while the S_d of solute Fe decreases from 0.47 to a minimum value of about 0.37. The decrease of segregation degree demonstrates that macrosegregation becomes increasingly obvious as undercooling increases. Besides, the Si concentration has been increased in the Fe-rich zone whereas reduced in the Cu-rich zone during the liquid phase separation.

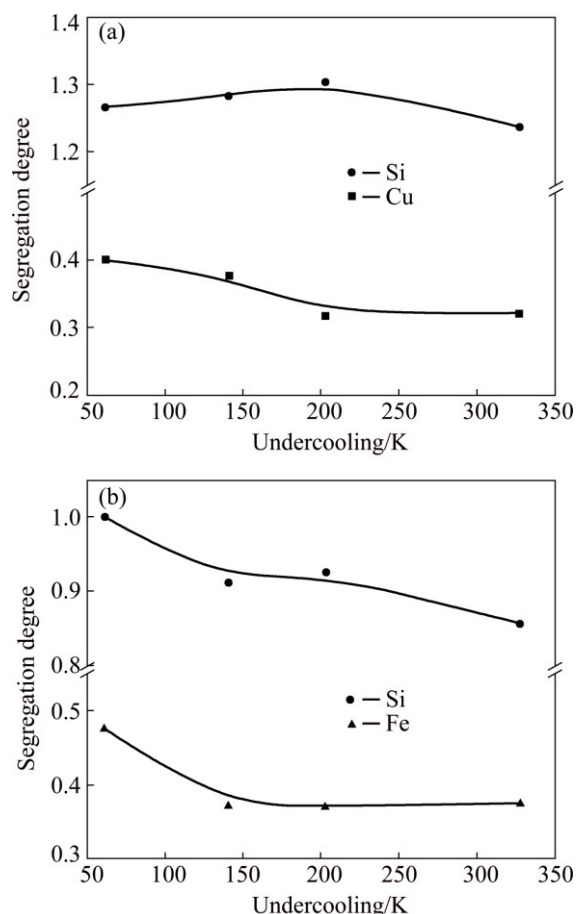


Fig. 3 Solute segregation degree of macrosegregated zones versus undercooling: (a) Fe-rich zone; (b) Cu-rich zone

Based on the results displayed in Fig. 1, α -Fe solid solution should be the primary phase of homogeneous liquid $\text{Fe}_{35}\text{Cu}_{35}\text{Si}_{30}$ alloy. Nevertheless, FeSi intermetallic compound will replace α -Fe phase as the primary phase if the macrosegregation occurs. Therefore, the solidification process of undercooled $\text{Fe}_{35}\text{Cu}_{35}\text{Si}_{30}$ alloy is significantly influenced by the variation of solute concentration, which is induced by liquid phase separation. X-ray diffractometry (XRD) analysis was performed to examine the phase constitution of the bulk alloy solidified after liquid phase separation. The XRD patterns are displayed in Fig. 4(a), in which θ is the diffraction angle. As a consequence, all of the phase-separated samples of ternary $\text{Fe}_{35}\text{Cu}_{35}\text{Si}_{30}$ alloy are composed of three phases: (Cu) solid solution, FeSi and Fe_5Si_3 intermetallic compounds.

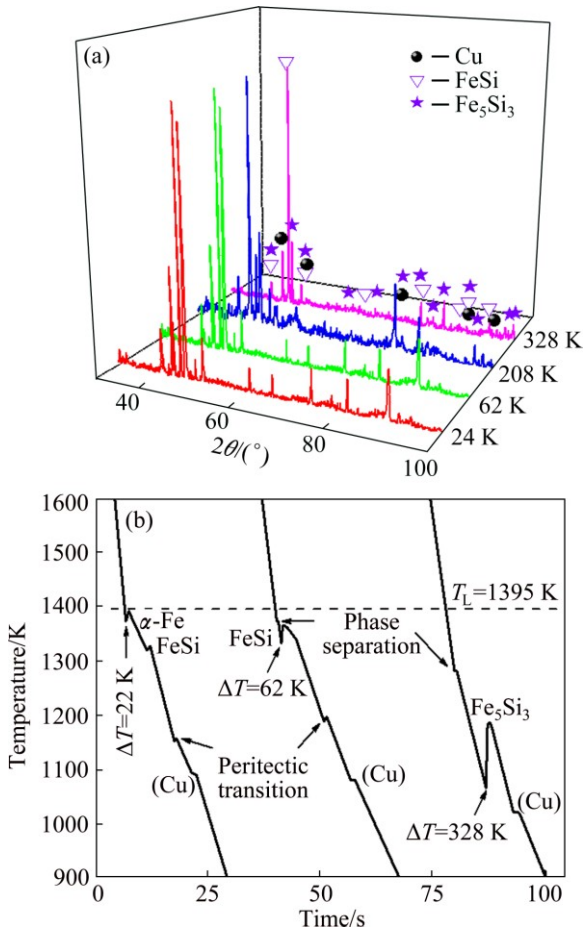


Fig. 4 XRD patterns (a) and typical cooling curves (b) of ternary Fe₃₅Cu₃₅Si₃₀ alloy

3.2 Dendritic solidification and microstructural evolution

Dendritic growth velocity is a very important parameter for investigating the solidification process. Since the primary phase of undercooled Fe₃₅Cu₃₅Si₃₀ alloy will change when the undercooling exceeds a certain value, it is necessary to quantitatively measure the dendritic growth velocity of the primary phase.

Dendritic growth velocity v equals the ratio of the growth distance L and the recalescence time t_{ps} , that is, $v=L/t_{ps}$. During the solidification of homogenous liquid alloy, the dendritic growth initiates from the sample bottom and travels all over the sample, as illustrated in Fig. 2(a). In this case, L could be taken as the sample length. For phase-separated alloy, the nucleation site is always at the segregation boundary and the Fe-rich zone is firstly solidified. At this point, L should be approximately regarded as the Fe-rich zone length.

As a critical parameter in the determination of growth velocity, recalescence time t_{ps} can be obtained from the cooling curve of alloy sample. Figure 4(b) displays the cooling curves of ternary Fe₃₅Cu₃₅Si₃₀ alloy

at three typical undercoolings. At the small undercooling of 22 K, there are four obvious recalescence peaks on the cooling curve. Based on the phase diagram and solidification microstructure, these four peaks correspond to the primary α -Fe phase growth, the second FeSi phase growth, the peritectic transition and the solidification of (Cu) phase, respectively. At the undercooling $\Delta T=62$ K, there are also four recalescence peaks on the cooling curve. Liquid phase separation takes place at $T=1373$ K, corresponding to the first peak. The following recalescence peak represents the rapid solidification of the primary FeSi phase starting at $T=1333$ K. The following two peaks represent the peritectic transition and the formation of (Cu) phase, respectively. For the cooling curve of the largest bulk undercooling, $\Delta T_{max}=328$ K, there are only three obvious recalescence peaks. According to the solidification microstructure, these three peaks should represent the liquid phase separation, the rapid growth of Fe₅Si₃ phase and the solidification of (Cu) phases, respectively.

Figure 5 gives the measured growth velocity v of primary phases in undercooled Fe₃₅Cu₃₅Si₃₀ alloy. When the undercooling is smaller than 24 K, α -Fe phase is the primary phase of homogeneous liquid Fe₃₅Cu₃₅Si₃₀ alloy. Its dendritic growth velocity rises almost linearly with increasing undercooling and obtains a value of about 17 mm/s at the undercooling of 23 K. The relationship of growth velocity versus undercooling is fitted as

$$v_{\alpha-Fe} = 11.17 + 0.11\Delta T \tag{2}$$

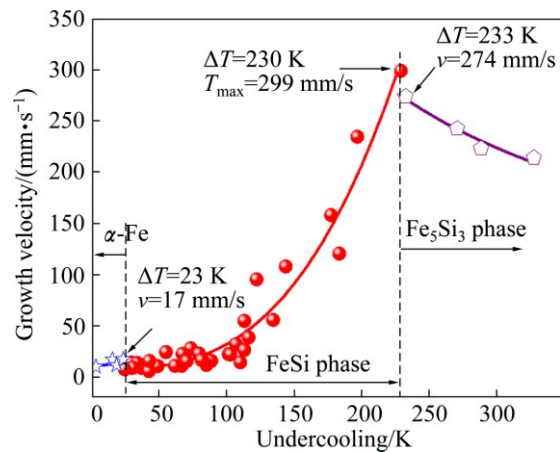


Fig. 5 Measured dendritic growth velocity of primary phases

If the undercooling exceeds 24 K, the FeSi intermetallic compound replaces α -Fe phase as the primary phase. This change is reflected by a slight reduction of growth velocity. At $\Delta T=24$ K, the growth velocity of the primary FeSi phase is only about 8 mm/s. Then, it rises rapidly with the enhancement of undercooling. At $\Delta T=230$ K, the growth velocity reaches the maximum value of 299 mm/s. In the undercooling

ranges of 24–230 K, the growth velocity of the primary FeSi phase follows a power law with undercooling:

$$v_{\text{FeSi}} = 7.76 + 2.22 \times 10^{-5} \Delta T^{3.02} \quad (3)$$

However, the growth velocity changes drastically once the undercooling exceeds 230 K. The growth velocity abruptly drops to 274 mm/s at the undercooling of 233 K, and subsequently decreases with increasing undercooling. In this case, the decreasing tendency of growth velocity can be expressed as

$$v_{\text{Fe}_5\text{Si}_3} = 1.71 \times 10^4 \Delta T^{-0.76} \quad (4)$$

The reason for the sudden variation of growth velocity is that Fe_5Si_3 phase replaces FeSi phase as the primary phase when the alloy is undercooled beyond 230 K. This is supported by the cooling curves shown in Fig. 4(b) and the solidification microstructure displayed in Fig. 6(c). The Fe_5Si_3 phase directly grows from the Fe-rich liquid as the primary phase in highly undercooled melts. Therefore, the measured dendritic growth velocity within the undercooling range of 230–328 K is actually that of Fe_5Si_3 phase. A possible explanation for the decrease in growth velocity is that the growth of Fe_5Si_3 phase is principally controlled by solutal diffusion. The solute diffuses more slowly at larger undercoolings.

It can be deduced from the measured results of dendritic growth velocity that the crystal growth within macrosegregated $\text{Fe}_{35}\text{Cu}_{35}\text{Si}_{30}$ alloy is very complex. Hence, the investigation of solidification microstructure is focused on the macrosegregated samples, the undercoolings of which are from 62 to 328 K in the present experiments.

Figure 6 presents the microstructural morphologies of the Fe-rich zone. When the undercooling is 62 K, the solidification microstructure of the Fe-rich zone is composed of FeSi, Fe_5Si_3 and (Cu) phases. Obviously, it is a typical peritectic-type morphology, as shown in Fig. 6(a). The peritectic transformation has proceeded to a large extent so that only a small quantity of primary FeSi phase remains in the peritectic Fe_5Si_3 phase. The latter appears as coarse grains without discernible dendrites. The (Cu) phase is randomly distributed inside the Fe-rich phase matrix. At $\Delta T=203$ K, the growth velocity of FeSi phase has increased to about 217 mm/s. Influenced by the rapid growth of FeSi phase, the peritectic Fe_5Si_3 phase appears as vermicular dendrites, as presented in Fig. 6(b). This demonstrates that remarkable microstructural refinement has taken place during rapid solidification. When the undercooling has increased to 328 K, the Fe-rich zone only consists of Fe_5Si_3 and (Cu) phases, as seen in Fig. 6(c). The peritectic solidification is suppressed completely and the primary Fe_5Si_3 phase directly grows from the Fe-rich liquid. Subsequently, the (Cu) phase crystallizes within

the residual liquid phase. In this case, the microstructural morphology of Fe_5Si_3 phase also shows vermicular dendrites.

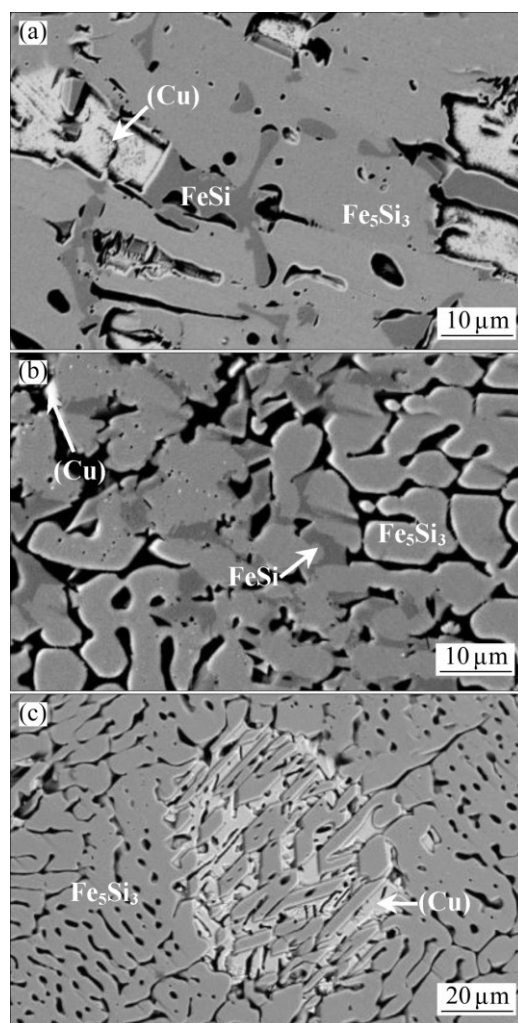


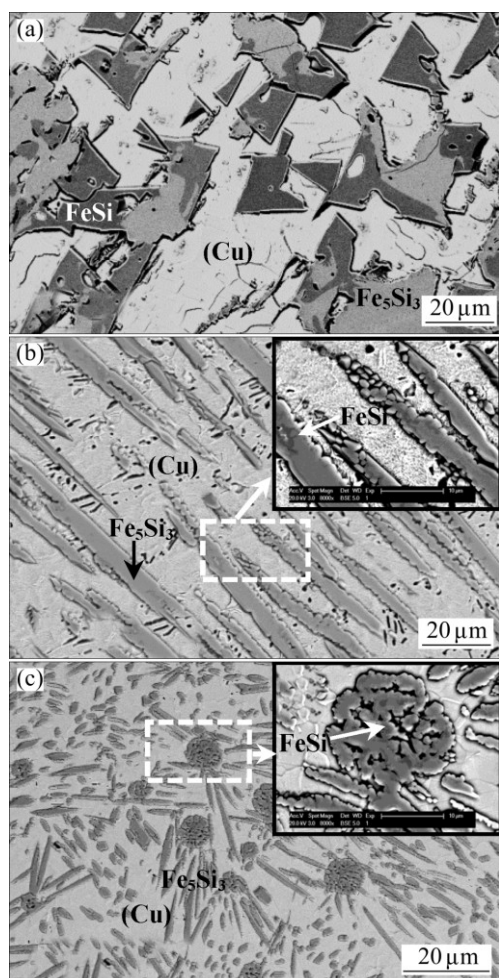
Fig. 6 Microstructural morphologies of Fe-rich zone at different undercoolings: (a) $\Delta T=62$ K; (b) $\Delta T=203$ K; (c) $\Delta T=328$ K

Table 1 gives the phase compositions of the Fe-rich zone at three typical undercoolings. It is obvious that FeSi phase has a lower Cu content than Fe_5Si_3 phase. The former has a value of only about 0.6%, while the latter is close to 3.0%. It is also noted that there is no distinct difference in Cu content between the peritectic Fe_5Si_3 phase and the primary Fe_5Si_3 phase. For the (Cu) solid solution phase, its Fe content rises from 1.89% to 3.96% when the undercooling ranges from 62 to 328 K, while the content of solute Si keeps a value of about 13.4%. Therefore, the solubility of solute Si was much more than that of solute Fe in the (Cu) phase.

Figure 7 displays the microstructural evolution of the Cu-rich zone. Clearly, the Cu-rich zone of macrosegregated $\text{Fe}_{35}\text{Cu}_{35}\text{Si}_{30}$ alloy is characterized by peritectic solidification at all undercoolings. At the

Table 1 Phase compositions of Fe-rich zone at different undercoolings (mole fraction, %)

Composition	$\Delta T=62$ K			$\Delta T=203$ K			$\Delta T=328$ K	
	FeSi	Fe ₅ Si ₃	(Cu)	FeSi	Fe ₅ Si ₃	(Cu)	Fe ₅ Si ₃	(Cu)
Fe	51.84	61.01	1.89	49.37	59.37	2.18	59.23	3.96
Cu	0.60	2.56	84.75	0.55	2.99	84.34	3.05	82.60
Si	47.56	36.43	13.36	50.08	37.64	13.47	37.72	13.34

**Fig. 7** Microstructural morphologies of Cu-rich zone at different undercoolings: (a) $\Delta T=62$ K; (b) $\Delta T=203$ K; (c) $\Delta T=328$ K

undercooling $\Delta T=62$ K, there still are a lot of primary FeSi phases remaining in the peritectic Fe₅Si₃ phase. The Fe₅Si₃ intermetallic compound appears as polygonal structure, as shown in Fig. 7(a). When the undercooling reaches 203 K, the Fe₅Si₃ phase is characterized by lath-like dendrites and a small number of spheres, as displayed in Fig. 7(b). Besides, only a trace amount of FeSi phase can be found in the Fe₅Si₃ phase. This means that the extent of the peritectic transformation has been improved. At the maximum undercooling $\Delta T_{\max}=328$ K, the Fe₅Si₃ phase still grows as a peritectic product, as illustrated in Fig. 7(c). This is different from the growth manner in the Fe-rich zone. The morphology of Fe₅Si₃

phase appears as spheres and lath-like dendrites.

The phase compositions of the Cu-rich zone are illustrated in Table 2. Obviously, all of the FeSi, Fe₅Si₃ and (Cu) phases display an extended solute solubility under substantial undercoolings. As the undercooling increases from 62 to 328 K, the Cu content of FeSi phase increases from 1.87% to 2.71%, and that of Fe₅Si₃ phase rises from 2.56% to 4.60%. For the (Cu) solid solution phase, the content ranges of the solutes Fe and Si are 1.24%–1.90% and 14.52%–17.12%, respectively.

Based on the experimental results, the solidification pathway of undercooled Fe₃₅Cu₃₅Si₃₀ alloy may be assumed as follows. It is divided into three stages according to the difference in alloy undercooling.

The first stage is 0–24 K undercooling. Below the critical undercooling of about 24 K, ternary Fe₃₅Cu₃₅Si₃₀ alloy solidifies as just like a normal homogenous alloy and α -Fe is the primary phase.

The second stage is 24–230 K undercooling. In this stage, the FeSi intermetallic compound is the primary phase. At the beginning, liquid phase separation occurs, that is, $L \rightarrow L_1(\text{Cu}) + L_2(\text{Fe})$. The $L_1(\text{Cu})$ and $L_2(\text{Fe})$ phases gradually gather together to form Cu-rich and Fe-rich zones, respectively. The Fe-rich zone solidifies firstly and plays a crucial role during the solidification of bulk alloy. The FeSi phase primarily nucleates and grows within the Fe-rich zone, and then reacts with the surrounding liquid to form Fe₅Si₃ phase. The peritectic transformation cannot be completely fulfilled under the non-equilibrium condition. Therefore, some primary FeSi phases remain in the peritectic Fe₅Si₃ phase, and the remnant liquid solidifies into (Cu) phase within interdendritic spacings. The Cu-rich zone solidifies in the same way as the Fe-rich zone.

The third stage is 230–328 K undercooling in the present work. In this solidification stage, the peritectic transformation is completely suppressed in the Fe-rich zone. The primary Fe₅Si₃ phase directly nucleates and grows from the Fe-rich liquid, and the remnant liquid solidifies into (Cu) phase.

4 Conclusions

1) Liquid Fe₃₅Cu₃₅Si₃₀ alloy has been undercooled by up to 328 K ($0.24T_1$) by the glass fluxing method, and it displays triple solidification mechanisms.

Table 2 Phase compositions of Cu-rich zone at different undercoolings (mole fraction, %)

Composition	$\Delta T=62$ K			$\Delta T=203$ K			$\Delta T=328$ K		
	FeSi	Fe ₅ Si ₃	(Cu)	FeSi	Fe ₅ Si ₃	(Cu)	FeSi	Fe ₅ Si ₃	(Cu)
Fe	49.97	61.87	1.24	49.20	58.31	1.73	50.00	57.49	1.90
Cu	1.87	2.56	84.24	2.60	3.64	81.89	2.71	4.60	80.98
Si	48.15	35.58	14.52	48.20	38.05	16.38	47.29	37.91	17.12

2) A small undercooling of 24 K is sufficient to induce a metastable liquid phase separation process. Then, the alloy melt separates into a Fe-rich top zone and a Cu-rich bottom zone. The average compositions of the separated zones deviate largely from the original alloy composition, which significantly influences the solidification process.

3) In the Fe-rich zone, FeSi intermetallic compound is the primary phase in the moderate undercooling regime below 230 K. The growth velocity of the primary FeSi phase rises with increasing undercooling, and its maximum value attains 299 mm/s. In this case, the solidification microstructure is characterized by peritectic-type morphology. If the undercooling exceeds 230 K, the peritectic solidification is suppressed completely and Fe₅Si₃ intermetallic compound directly grows from the Fe-rich liquid as the primary phase. The growth velocity of the primary Fe₅Si₃ phase reduces with increasing undercooling, since its growth is principally controlled by solutal diffusion.

4) In the Cu-rich zone, FeSi intermetallic compound is always the primary phase at all of the undercoolings. The morphology of the Cu-rich zone appears as polygonal structures in the condition of small undercooling, whereas it is characterized by spheres and lath-like dendrites in the highly undercooled regime.

5) EDS results indicate that Fe₅Si₃ phase has a larger Cu content than FeSi phase. For the (Cu) solid solution phase, the solubility of solute Si is much more than that of solute Fe.

Acknowledgements

The authors acknowledge Dr. J. CHANG, Dr. L. HU, Dr. D. L. GENG and Mr. S. WANG for their technical assistance and helpful discussions.

References

- [1] HE J, MATTERN N, TAN J, ZHAO J Z, KABAN I, WANG Z, RATKE L, KIM D H, KIM W T, ECKERT J. A bridge from monotectic alloys to liquid-phase-separated bulk metallic glasses: Design, microstructure and phase evolution [J]. *Acta Materialia*, 2013, 61: 2102–2112.
- [2] YANG Gen-cang, XIE Hui, HAO Wei-xin, ZHANG Zhong-ming, GUO Xue-feng. Liquid–liquid phase separation in highly undercooled Ni–Pb hypermonotectic alloys [J]. *Transactions of Nonferrous Metals Society of China*, 2006, 16: 290–293.
- [3] SCHMITZ S, LINDENKREUZ H G, MATTERN N, LÖSER W, BÜCHNER B. Liquid phase separation in Gd–Ti and Gd–Zr melts [J]. *Intermetallics*, 2010, 18: 1941–1945.
- [4] CURIOTTO S, PRYDS N H, JOHNSON E, BATTEZZATI L. Liquid–liquid phase separation and remixing in the Cu–Co system [J]. *Metallurgical and Materials Transactions A*, 2006, 37: 2361–2368.
- [5] EGRY I, RATKE L, KOLBE M, CHATAIN D, CURIOTTO S, BATTEZZATI L, JOHNSON E, PRYDS N. Interfacial properties of immiscible Co–Cu alloys [J]. *Journal of Materials Science*, 2010, 45: 1979–1985.
- [6] LUO S B, WANG W L, CHANG J, XIA Z C, WEI B. A comparative study of dendritic growth within undercooled liquid pure Fe and Fe₅₀Cu₅₀ alloy [J]. *Acta Materialia*, 2014, 69: 355–364.
- [7] REITH D, PODLOUCKY R. First-principles model study of the phase stabilities of dilute Fe–Cu alloys: Role of vibrational free energy [J]. *Physical Review B*, 2009, 80: 054108.
- [8] ZHAO L, ZHAO J Z. Rapid solidification behavior of Cu–Co–Fe alloy [J]. *Journal of Materials Research*, 2013, 28: 1203–1210.
- [9] GUO Jin-bo, CAO Chong-de, GONG Su-lian, SONG Rui-bo, BAI Xiao-jun, WANG Jian-yuan, ZHENG Jian-bang, WEN Xi-xing, SUN Zhan-bo. Rapid solidification of Cu₆₀Co₃₀Cr₁₀ alloy under different conditions [J]. *Transactions of Nonferrous Metals Society of China*, 2013, 23: 731–734.
- [10] HINO M, NAGASAKA T, WASHIZU T. Phase diagram of Fe–Cu–Si ternary system above 1523 K [J]. *Journal of Phase Equilibria*, 1999, 20: 179–186.
- [11] RAGHAVAN V. Cu–Fe–Si (Copper–Iron–Silicon) [J]. *Journal of Phase Equilibria*, 2002, 23: 267–270.
- [12] MIETTINEN J. Thermodynamic description of the Cu–Fe–Si system at the Cu–Fe side [J]. *Calphad*, 2003, 27: 389–394.
- [13] VILLARS P, PRINCE A, OKAMOTO H. Handbook of ternary alloy phase diagrams [M]. Ohio: ASM International, 1995: 9444–9453.
- [14] QUE Zhong-ping, GU Ji-Ho, SHIN Jong-Ho, LEE Je-Hyun. Microstructure transition from stable to metastable eutectic growth in Ni–25%Al alloy [J]. *Transactions of Nonferrous Metals Society of China*, 2014, 24(S1): s106–s111.
- [15] LIU X J, CHEN G L, LI F, HUI X D, LU Z P, YE F, LIU C T. Evolution of atomic ordering in metallic glasses [J]. *Intermetallics*, 2010, 18: 2333–2337.
- [16] CASTLE E G, MULLIS A M, COCHRANE R F. Mechanism selection for spontaneous grain refinement in undercooled metallic melts [J]. *Acta Materialia*, 2014, 77: 76–84.
- [17] BALOYI N M, POPOOLA A P I, PITYANA S L. Microstructure, hardness and corrosion properties of laser processed Ti6Al4V-based composites [J]. *Transactions of Nonferrous Metals Society of China*, 2015, 25: 2912–2923.
- [18] LUO S B, WANG W L, XIA Z C, WU Y H, WEI B. Solute redistribution during phase separation of ternary Fe–Cu–Si alloy [J]. *Applied Physics A*, 2015, 119: 1003–1011.
- [19] SOBOLEV S L. An analytical model for local-nonequilibrium solute trapping during rapid solidification [J]. *Transactions of Nonferrous Metals Society of China*, 2012, 22: 2749–2755.
- [20] NAYAK S S, CHANG H J, KIM D H, PABI S K, MURTY B S. Formation of metastable phases and nanocomposite structures in rapidly solidified Al–Fe alloys [J]. *Materials Science and*

- Engineering A, 2011, 528: 5967–5973.
- [21] LI Sheng, WANG Hai-feng, LIU Feng. Microstructure and microtexture evolution of undercooled Ni–15%Cu alloy [J]. Transactions of Nonferrous Metals Society of China, 2013, 23: 3265–3270.
- [22] CAO L G, COCHRANE R F, MULLIS A M. Solidification morphology and phase selection in drop-tube processed Ni–Fe–Si intermetallics [J]. Intermetallics, 2015, 60: 33–44.
- [23] SHULESHOVA O, WOODCOCK T G, LINDENKREUZ H G, HERMANN R, LÖSER W, BÜCHNER B. Metastable phase formation in Ti–Al–Nb undercooled melts [J]. Acta Materialia, 2007, 55: 681–689.
- [24] JOHNSON M L, MAURO N A, VOGT A J, BLODGETT M E, PUEBLO C, KELTON K F. Structural evolution and thermophysical properties of Zr_xNi_{100-x} metallic liquids and glasses [J]. Journal of Non-crystalline Solids, 2014, 405: 211–218.
- [25] XIA Z C, WANG W L, LUO S B, WEI B. Liquid phase separation and rapid dendritic growth of highly undercooled ternary $Fe_{62.5}Cu_{27.5}Sn_{10}$ alloy [J]. Journal of Applied Physics, 2015, 117: 054901.
- [26] PLEVACHUK Y, SKLYARCHUK V, ALEKHIN O, BILOUS O. Viscosity of liquid binary Pb–Zn alloys in the miscibility gap region [J]. Journal of Non-crystalline Solids, 2014, 391: 12–16.

深过冷三元 $Fe_{35}Cu_{35}Si_{30}$ 合金的 液相分离与枝晶生长特征

罗盛宝, 王伟丽, 夏瑛超, 魏炳波

西北工业大学 应用物理系, 西安 710072

摘 要: 采用熔融玻璃净化技术研究了三元 $Fe_{35}Cu_{35}Si_{30}$ 合金的液相分离与枝晶生长特征。实验获得的最大过冷度为 328 K ($0.24T_L$)。结果表明, 合金在深过冷条件下具有三重凝固机制。当过冷度小于 24 K 时, α -Fe 相为初生相, 凝固组织为均匀分布的枝晶。过冷度超过 24 K 之后, 合金熔体分离为富 Fe 区和富 Cu 区。在过冷度低于 230 K 的范围内, FeSi 金属间化合物为富 Fe 区的初生相; 当过冷度高于 230 K 时, Fe_5Si_3 金属间化合物取代 FeSi 相成为富 Fe 区的初生相。随着合金过冷度的增加, FeSi 相的生长速率逐渐升高, 而 Fe_5Si_3 相的生长速率将逐渐降低。在富 Cu 区, 初生相始终为 FeSi 金属间化合物。能谱分析表明, 富 Fe 区和富 Cu 区的平均成分均已严重偏离初始合金成分。

关键词: 深过冷; 相分离; 枝晶生长; 快速凝固; 溶质分布

(Edited by Yun-bin HE)